Arabian Journal for Science and Engineering (2019) 44:1917–1931
https://doi.org/10.1007/s13369-018-3188-0

RESEARCH ARTICLE - ELECTRICAL ENGINEERING

Design of Digital Differentiator Using the L_1-Method and Swarm Intelligence-Based Optimization Algorithms

Apoorva Aggarwal[1] · Manjeet Kumar[2] · T. K. Rawat[3]

Received: 6 November 2017 / Accepted: 19 March 2018 / Published online: 29 March 2018

Abstract
In this paper, a novel approach to design the digital linear-phase finite impulse response (FIR) differentiator is introduced. First, the differentiator design problem is formulated using the L_1-method. Then, the L_1 optimality criterion is applied using the Bat algorithm (BA) and Particle swarm optimization (PSO) to further optimize the differentiator design. A novel fitness function is developed based on the L_1-error norm which is unique and is liable to produce a flat response. These techniques are developed in order to minimize the non-differentiable fitness function. Finally, the simulation results have been presented for 5th-, 7th- and 11th-order FIR differentiator using the L_1-method, PSO-L_1 and BA-L_1. The magnitude response of the designed differentiators is analyzed for different frequency bands on the basis of relative magnitude error computed with respect to the ideal response. All the reported techniques contribute toward superior results, when compared with the traditional gradient-based optimizations, such as the window method, minimax and least-squares approach. In addition, the L_1-method yields better results for higher-order designs. Furthermore, the proposed designs are tested on two input signals for their efficient response.

Keywords Finite impulse response · L_1-error criterion · Digital differentiator · Bat algorithm · Particle swarm optimization

1 Introduction

The design of digital differentiators (DD) is an emerging area of research in the field of signal processing. DD is practiced for extracting the information about rapid transients by calculating the time derivative of the input signal. DDs are applied in a variety of applications such as in the field of radar and sonar signal processing, speech and image processing, communication systems, control engineering, biomedical engineering and seismic signal processing [1–10]. The frequency response of an ideal DD is $j\omega$, where $j = \sqrt{-1}$ and ω is the digital angular frequency in radians for the range, $[0, \pi]$.

Traditionally, the DD have been designed by making suitable modifications after inverting the response of the various existing integrators. In the beginning, simple interpolation-based approaches were adopted in order to obtain the recursive differentiators [11–15]. In [11,12], Al-Alaoui and Bihan proposed a novel integrator and differentiator by interpolating both, the rectangular and trapezoidal integration rules, which resulted in a better approximate to the ideal ones. Al-Alaoui in 1994 employed the Simpson integration rule to obtain a stable second-order infinite impulse response (IIR) differentiator with high accuracy and almost linear phase at lower frequencies [13]. In 2011, Al-Alaoui proposed the digital integrator and differentiator derived by interpolating different weighted combinations of Simpson, trapezoidal and Boole rules which leads to various segments and further optimized them using simulated annealing (SA) [14]. Gupta et al. [15] interpolated three digital integration techniques to design third-order integrator and differentiator of high accu-

✉ Manjeet Kumar
manjeetchhillar@gmail.com

Apoorva Aggarwal
16.apoorva@gmail.com

T. K. Rawat
tarundsp@gmail.com

[1] Department of Electrical and Electronics Engineering, Bharati Vidyapeeths College of Engineering, New Delhi 110063, India

[2] Department of Electronics and Communication Engineering, Bennett University, Greater Noida, Uttar Pardesh 201310, India

[3] Department of Electronics and Communication Engineering, Netaji Subhas Institute of Technology, Dwarka, Delhi 110078, India

racy. Besides, a linear programming to approximate the ideal integrator in minimax sense was proposed in [16]. Ngo [17] applied the Newton-Cotes integration rule for the deign of wideband digital operators.

In recent years, the design procedure of DD and integrator has been evolved as an optimization problem. It is due to the fact that the evolutionary and swarm intelligence (SI)-based optimization algorithms are capable of solving multimodal, non-linear and non-differentiable complex problems [18,19]. A novel recursive differentiator and integrator was obtained by the pole zero optimization method suitable for the real-time applications [20,21]. A linear-phase second-order IIR integrator and differentiator was introduced by Jain et al. [22] using genetic algorithm (GA) to minimize the absolute relative error. To date, the PSO algorithm was successfully applied for the design of digital IIR integrator and higher-order FIR differentiator [23,24]. IIR differentiator was designed using SA, GA and Fletcher and Powell optimization by Al-Alaoui and Baydoun [25] to obtain the results with high accuracy.

In digital signal processing, the digital systems are mainly of two types, finite impulse response (FIR) and infinite impulse response (IIR) [26]. In FIR systems, the system output depends only on the past and present inputs, and hence these systems are realized non-recursively, whereas IIR systems are realized recursively and their output is influenced by the past and present inputs along with the past outputs. Some of the advantages of FIR systems over IIR are summarized below.

1. The FIR systems have the linear phase characteristics due to the symmetric and anti-symmetric impulse response. This reduces the complexity in solving the optimization problem. The characteristics of linear phase provide a constant delay to the input signal which makes it suitable for real-time applications.
2. The FIR structures are implemented by direct convolution and can be realized non-recursively.
3. Since all poles lie on the origin hence, FIR systems are inherently stable.

With these advantages of FIR systems, the design of FIR differentiator with anti-symmetric impulse response is considered in this work, using the L_1-optimality criterion. The applicability of the L_1-norm is common in engineering applications [27,28]. But, it was unexplored in the field of signal processing and system design due to the limitation of non-differentiability. The L_1-method was developed for the design of linear phase FIR filters by Grossmann and Eldar [29] which exploited the problems of differentiability and unique results while using the L_1-norm. The motivation behind using the L_1-criterion for the optimization purposes is summarized below.

1. In comparison to the least-squares (LS) and minimax design methods, it is observed that using the L_1-norm yields the smallest overshoot at the edges in ideal response [29].
2. The L_1-based filter possesses a flat passband and stopband along with sharp transitions.
3. An efficient L_1-method is being developed for its successful application in the computation of system parameters.

Till date, the L_1-method with the above advantages, is not being applied for the design of FIR differentiators. In this paper, the design of digital 5th-, 7th- and 11th-order FIR differentiator is considered using different optimization approaches such as the L_1-method, PSO and BA based on the L_1-optimality criterion. A wideband differentiator is designed and analyzed over different frequency bands for each technique. Moreover, the design results are further compared with the traditional differentiator design techniques, the window methods, minimax and LS approach. On the basis of the observations made on absolute magnitude error obtained in different frequency bands, the L_1-method provides substantially better results in the range $[0, 0.8\pi]$ for the higher-order differentiator, whereas for the complete frequency range, differentiator designed using BA-L_1 exhibits better performance.

The formulation of the paper is as follows: Sect. 2 defines the FIR differentiator design problem. A brief overview of the design methods implemented in this work is presented in Sect. 3. In Sect. 4, the simulation results are demonstrated for the design of FIR differentiator using the L_1-method, PSO-L_1 and BA-L_1. A detailed analysis and comparison is carried out with the existing methods. Section 5 concludes the work.

2 Wideband FIR Differentiator Design Problem

This section formulates the design problem of digital Nth-order FIR differentiator by approximating it to the response of an ideal differentiator. An ideal differentiator prototype is characterized by the frequency response given by

$$D(\omega) = \jmath\omega, \qquad -\pi \leq \omega \leq \pi \tag{1}$$

where ω represents the digital angular frequency. The frequency response of ideal differentiator in Eq. (1) is approximated to the Nth-order FIR digital filter which is inherently stable. The approximating filter frequency response $H(\omega)$ is obtained by the discrete time Fourier transform of the filter impulse response, $h[n]$, $0 \leq n \leq N$ given by

$$H(\omega) = \sum_{n=0}^{N} h[n] \mathrm{e}^{-j\omega n} \tag{2}$$

To design a full-band differentiator, the type-IV linear-phase FIR filter with even length and anti-symmetric coefficients is considered. The condition for anti-symmetrical coefficients implies $h[n] = -h[N-n], 0 \leq n \leq N$. The frequency response of type-IV FIR filter is given by [26]

$$H(\omega) = \mathrm{e}^{j(\frac{\pi}{2} - \omega M)} \sum_{n=1}^{M} d[n] \sin(\omega (n - 0.5)) \tag{3}$$

where $M = (N-1)/2$ and $d[n] = 2h[M-n], 1 \leq n \leq M$, are the filter coefficients. The amplitude response of the type-IV FIR filters is given by

$$H_r(\omega) = \sum_{n=1}^{M} d[n] \sin(\omega (n - 0.5)) \tag{4}$$

The error function, $E(\omega)$, is articulated to approximate the amplitude response, $H_r(\omega)$, to the ideal frequency response. The error objective function based on the L_1-norm is expressed as

$$||E(\omega)||_1 = \sum_{\omega} |H_r(\omega) - D(\omega)| \tag{5}$$

The implementation of objective function in the L_1-sense delivers the flattest response among others, such as the L_2 and L_∞-norms. Thus, using the L_1-error criterion with the SI based optimization algorithms, BA and PSO for the design of digital FIR differentiator have advantage of obtaining the flat frequency response.

In this work, the error function given in Eq. (5) is employed as the objective function for the optimization problem. Constructing it as a minimization problem, this function is minimized using the L_1-method, PSO-L_1 and BA-L_1 optimization techniques and the corresponding optimized anti-symmetric filter coefficients are used for the design of 5th-, 7th- and 11th-order digital FIR differentiator.

3 The Digital FIR Differentiator Design Methodologies

In this section, the methods implemented for the design of digital FIR differentiator are described in detail. The optimal design of differentiator involves the computation of FIR filter coefficients approximated to the ideal differentiator response by minimizing the error function based on L_1-norm. The L_1-method is applied to design the FIR differentiator with linear phase characteristics, stable system and a flat response over the complete frequency range. Further, the PSO and BA are executed to obtain more optimized filter coefficients with the constraints of differentiator response. The steps exercised by the L_1-method, PSO and BA for the design problem are as follows.

3.1 The L_1-Method for the Design of Digital FIR Differentiator

The L_1-method, based on the L_1-optimality criteria, was explored to be utilized in the FIR system design processes. In 2007, Grossmann and Eldar successfully exploited the problem of differentiability and uniqueness in the design of FIR filters using the L_1-algorithm based on modified Newton's method [29]. The L_1-fitness function results in a small overshoot and a flat passband profile as compared with the optimality criteria, minimax and LS. The design of FIR filters using the L_1-method and its characteristic comparison with the minimax technique is presented in [30–35]. This method is described here, for the design of FIR differentiator.

The algorithm applied to formulate the L_1 problem as a linear approximation problem demands for the evaluation of first- and second-order derivative of the error function defined in Eq. (5). The first-order derivative of the error function (the nth component) with respect to the system coefficients is given by [29]

$$g_n(\mathbf{d}) = \langle \cos(n\omega), \mathrm{sgn}(E(\omega, \mathbf{d})) \rangle \tag{6}$$

where $\mathrm{sgn}(E(\omega, \mathbf{d}))$ gives the Signum result of the function $E(\omega, \mathbf{d})$ and $\mathbf{d}$ is the coefficient vector $d[n], 1 \leq n \leq M$.

The steps for the implementation of the digital FIR differentiator using the L_1-method are articulated below.

Step 1: Initialization Design the ideal frequency response defined in (1). Set stopping condition factor, ϵ, step-size selection parameters, σ, β and the control parameters of Hessian matrix (second-order derivative of error function), δ_1, δ_2 and μ.

Step 2: Compute Determine the Hessian matrix over the entire digital frequency, given by

$$\mathbf{H}(\mathbf{d}) = \mathbf{R}^{\mathrm{T}} \mathbf{A}^{-1} \mathbf{R} \tag{7}$$

where $\mathbf{R}$ is a $t \times M$ matrix with $\mathbf{R}_{ij} = \cos((j-0.5)z_i)$, $t =$ number of zeros of $(E(\omega, \mathbf{d}))$ and z_i denotes the location of zeros of $E(\omega, \mathbf{d})$ at ith position, equal to $\frac{(2i-1)\pi}{2M}$, $i = 1, 2, \ldots, t$. $\mathbf{A} = \mathrm{diag}\{a_1, \ldots, a_t\}$ with $a_i = \frac{2(z_i)}{E'(\omega, \mathbf{d})}$.

Step 3: Compare The Hessian matrix, $\mathbf{H}^l$ of size $M \times M$ in Eq. (7) takes one of three forms according to the number of zeros of $E(\omega, \mathbf{d})$ to reduce the computations.

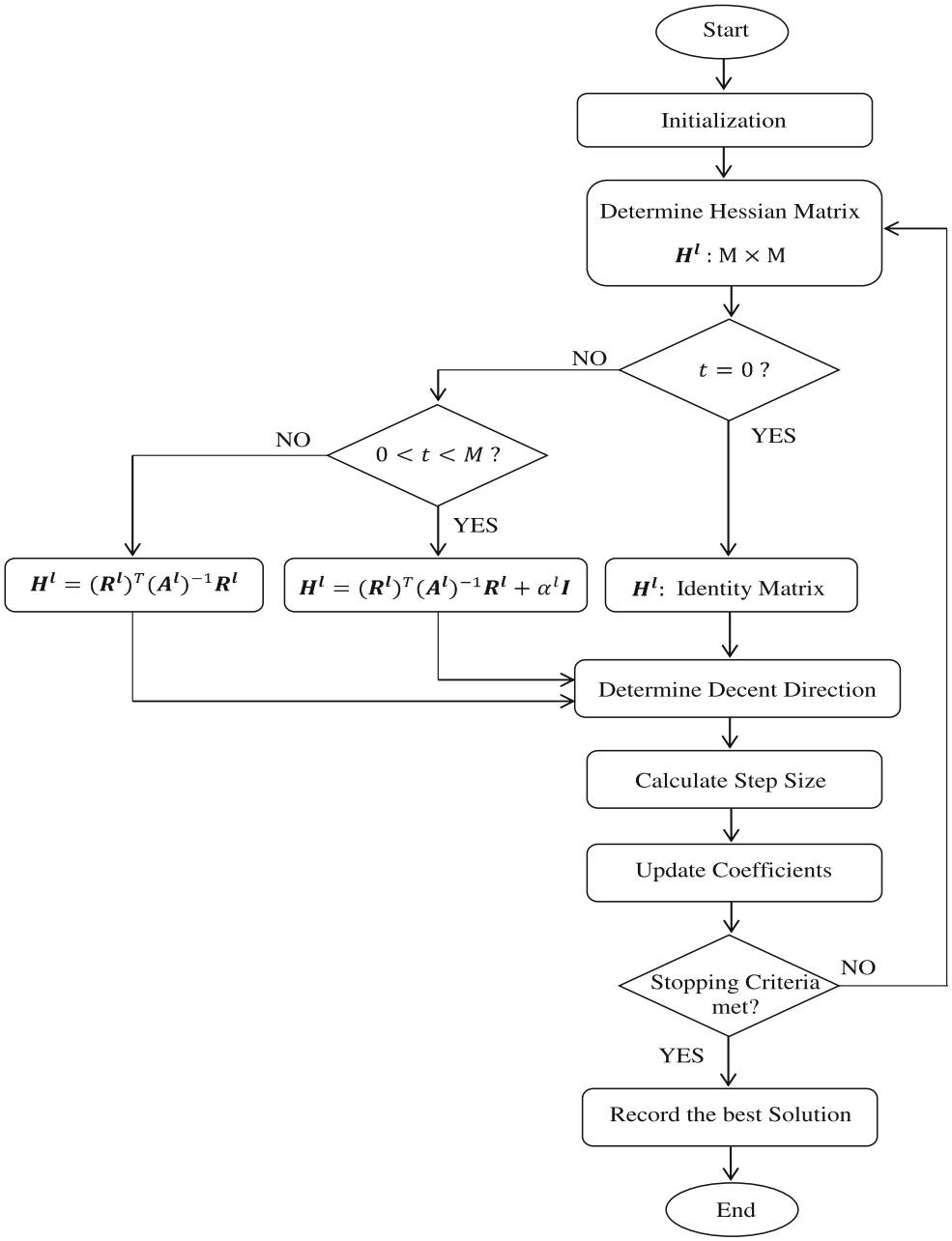

Fig. 1 Flowchart for the L_1 based FIR wideband differentiator design method

(i) If $t = 0$ or $\mathbf{A}$ is singular, then set Hessian matrix as identity matrix.
(ii) If $t \geq M$, $\mathbf{A}$ is non-singular and rank $\mathbf{R}^l = M$, then set $\mathbf{H}^l = (\mathbf{R}^l)^{\mathrm{T}}(\mathbf{A}^l)^{-1}\mathbf{R}^l$.
(iii) If $0 < t < M$, $\mathbf{A}$ is non-singular and rank $\mathbf{R}^l < M$, then set $\mathbf{H}^l = (\mathbf{R}^l)^{\mathrm{T}}(\mathbf{A}^l)^{-1}\mathbf{R}^l + \alpha^l \mathbf{I}$, where $\alpha^l > 0$ is the step size, determined according to the Armijo rule [36].

Step 4: Direction Determine the descent direction $\mathbf{k}^l$ to obtain the unique solution, given by

$$\mathbf{k}^l = -[\mathbf{H}^l]^{-1}\mathbf{g}^l \tag{8}$$

where $\mathbf{g^l}$ is the gradient [matrix form of Eq. (6)] of function at $\mathbf{d}^l$. Solving $\mathbf{k}^l$ also called the gradient method, involves the solution of the linear equations with M unknowns (the length of $\mathbf{k}^l$).

Step 5: Update Stop if $|(\mathbf{k}^l)^{\mathrm{T}}\mathbf{g^l}|$ is less than the given threshold, ϵ. Set $\mathbf{d}^{l+1} = \mathbf{d}^l + \alpha^l \mathbf{k}^l$ and $l = l + 1$. Goto Step 2.

Step 6: Record The M coefficients, $d[n]$, are stored, and the frequency response of designed Nth-order FIR differentiator is calculated.

The process flow chart for the L_1-method is pictured in Fig. 1.

3.2 PSO Algorithm to Optimize the Digital FIR Differentiator

PSO algorithm is the mathematical modeling of the behavior of certain animals working in a team such as fish schooling, insect swarming and bird flocking. This scenario is transformed into an artificial swarm, and a population-based stochastic search technique is developed [37]. This optimization algorithm is successfully being applied worldwide and is found to be robust and also suitable for non-differentiable and multiple objective functions. The algorithm enables each particle to act as a potential solution and is assigned with its position vector in the solution space, along with a velocity quotient with which it moves toward the optimal solution. At every iteration, the fitness value of each particle is eval-

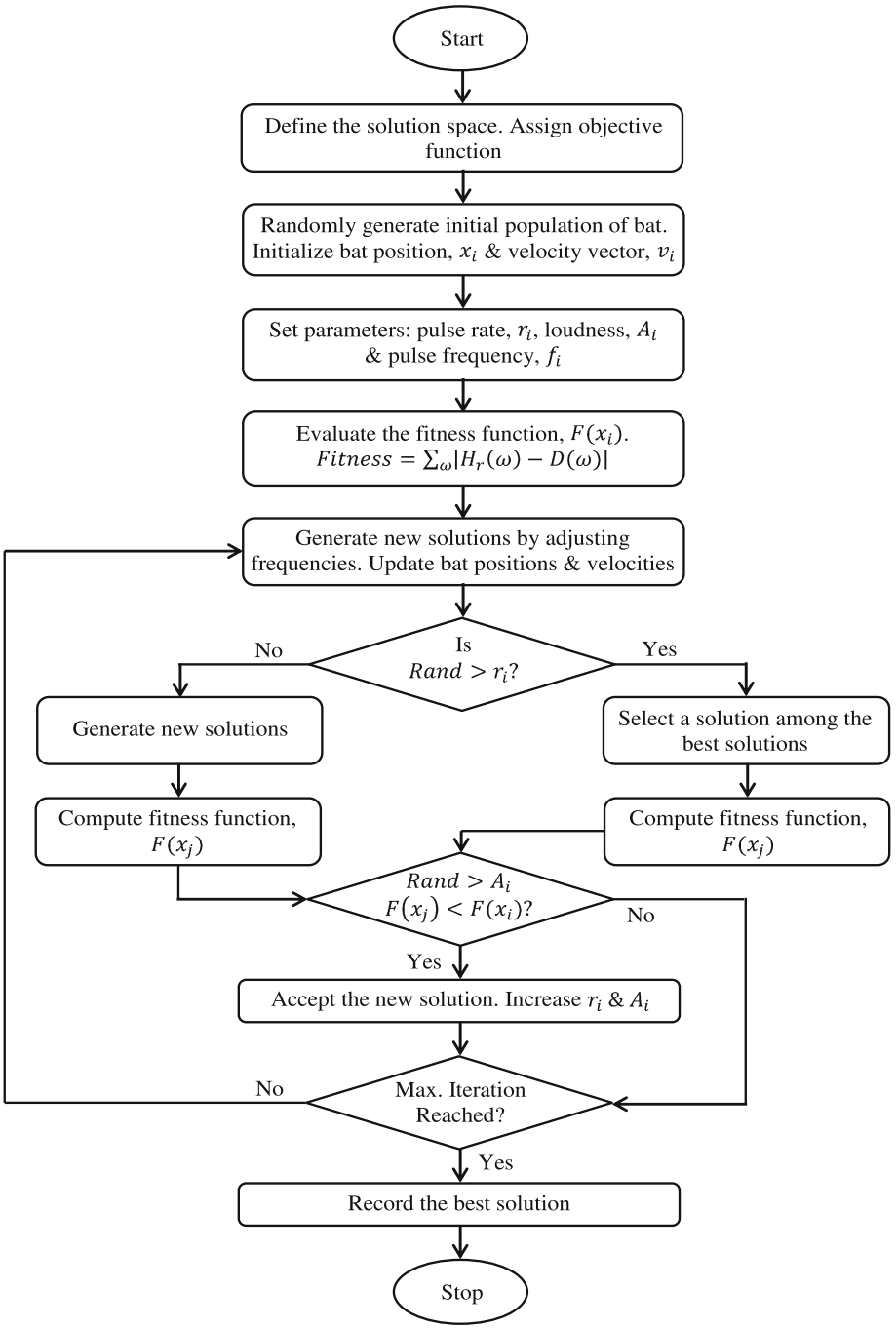

Fig. 2 Flowchart of the BA for the FIR differentiator design

Table 1 Control parameters of optimization algorithms for FIR DD design

Parameters	Symbol	L_1-method	PSO	BA
Tolerance	ϵ	10^{-6}	10^{-6}	10^{-6}
Step-size selection	σ, β	$10^{-3}, 0.5$	–	–
Hessian matrix control	δ_1, δ_2, μ	$10^{-15}, 10^{15}, 10^{-10}$	–	–
Initial population	n_i	–	55	25
Lower bound	$L_{\min}$	–	-1	-1
Upper bound	$L_{\max}$	–	1	1
Maximum iterations	–	–	100	100
Cognitive constant	C_1	–	2.0	–
Social constant	C_2	–	2.0	–
Initial velocity	$v_i^{\min}$	–	0.01	–
Final velocity	$v_i^{\max}$	–	1.0	–
Loudness	A_i	–	–	0.5
Pulse rate	r_i	–	–	0.5
Lower frequency (for BA)	$f_{\min}$	–	–	0
Higher frequency (for BA)	$f_{\max}$	–	–	2
Stopping criteria	–	Tolerance	Maximum iteration	Maximum iteration

Table 2 Optimized coefficients of 5th-order FIR differentiator using different optimization techniques

Technique	$h(0) = -h(5)$	$h(1) = -h(4)$	$h(2) = -h(3)$
Bartlett	0.00000000000001	0.06002108774380	-0.36012652646284
Hamming	0.00720253052925	0.05969880190037	-0.41061078138177
Minimax	-0.05241903529644	0.02499564645007	0.41391158430352
Least-squares	0.00676208592350	-0.03798136206270	0.41722262201710
L_1-method	0.02420857648777	-0.12341448837397	1.25834227136554
PSO-L_1	-0.01138089089321	0.04100798597085	-0.40220639775600
BA-L_1	-0.01106293662801	0.04121028263836	-0.40200282632863

uated and it is attracted toward the position of the current global best location. The steps implemented for the design of PSO-based FIR differentiator are summarized.

Step 1: Initialization Set the following parameters of the algorithm. Swarm size of the particle, n_i, maximum number of iterations, learning parameters, C_1, C_2 and limit of solution space.

Step 2: Initial Generation Randomly generate particle population with the initial position and velocity vectors, $x_i, v_i, i = 1, 2, \ldots, n$, respectively. Measure the fitness for each particle.

Step 3: Define Assign the variables, $pbest$, particle's personal best value and $gbest$, the global best position vector at the current iteration, l, with all the fitness values computed in Step 2.

Step 4: Movement The velocity and position vectors of each particle are updated for the next iteration according to the following equations considering the initial velocity of the ith particle, $v_i^{l=0} = 0$.

$$v_i^{l+1} = W * v_i^l + \alpha * C_1 * [gbest^l - x_i^l] + \beta * C_2 * [pbest_i^l - x_i^l] \quad (9)$$

$$x_i^{l+1} = x_i^l + v_i^{l+1} \quad (10)$$

where W is the inertia weight parameter that controls the tradeoff between $gbest$ and $pbest$ of the swarm. Also, C_1, C_2 are the cognitive and social parameters, respectively, that indicate the relative attraction toward $gbest$ and $pbest$ and α, β ranges between [0, 1]. The velocity quotient is bounded with $v_{\min}, v_{\max}$. With the iterations, the particle continuously shifts and ultimately reaches the global best solution which becomes the optimal solution obtained by PSO.

Step 5: Compare Calculate fitness of all the new solutions and modify $pbest$ and $gbest$ on basis the of updated fitness values.

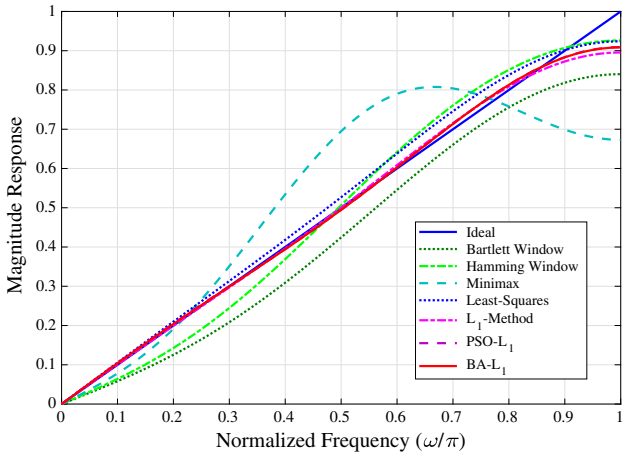

Fig. 3 Magnitude response of 5th-order FIR differentiator using different techniques over complete digital frequency range

Step 6: Solution Repeat steps 4–6 until the maximum number of iterations has reached. The final value of *gbest* obtained is the optimized solution. The process flow of the PSO algorithm is explained in Fig. 2.

3.3 Bat Algorithm to Optimize the Digital FIR Differentiator

A new metaheuristic algorithm, inspired from the natural echolocation behavior of the microbats, was developed by Yang in 2010 [38]. The bat algorithm is population-based stochastic search approach for solving constrained optimization problem with the multimodal fitness function. The echolocation process performed by bats investigates the presence of prey for their survival. It allows them to sense nearby movements and vibrations, even in the dark. It is similar to the principles of sonar signaling where the bat emits very high frequency sound waves and learns back from the reflected echoes. They account for three parameters, (1) time delay between the transmitted and detected waves, (2) time difference between their ears and (3) the variation in loudness, to create a three-dimensional perception of the environment. With these parameters, they inherently determine the obstacle/target size, distance and direction from the target, its speed and texture. With the efficient performance of BA, it has been applied in various applications, such as image processing, feature selection, data mining, parameter estimation and many other engineering optimization problems [39–47].

The algorithm follows some idealistic rules for its successful operation.

1. The bats use their inherent magical potential to classify between an obstacle and prey, in their path.
2. In the process of searching, bat flies randomly with velocity, $\mathbf{v}_i$ to achieve the position $\mathbf{x}_i$, with a fixed frequency $f_{\min}$, variable wavelength, λ and a loudness parameter, A_0. Based on the propinquity of the target, bats reflex toward adjusting the wavelength of emitting waves and the pulse rate, $r \in [0, 1]$.
3. The loudness values can be constant or decreasing from a maximum limit.
4. There is limit to the maximum and minimum frequency/wavelength of emitting waves.

In order to formulate BA according to the FIR DD problem, the implementation steps are as follows. The algorithm flow is projected in Fig. 2 in the form of a flowchart.

Step 1: Initialization Set population size of bats, n_i, maximum number of iterations, number of parameters to be

Table 3 Absolute magnitude error over complete frequency range for 5th-, 7th- and 11th-order differentiator using different optimization techniques

Order	Bartlett window	Hamming window	Minimax technique	Least-squares	L_1-method	PSO-L_1	BA-L_1
5	21.0862	12.0760	34.6911	7.4261	3.5148	3.2451	**3.2373**
7	22.8349	28.2085	37.2930	14.3325	3.8943	1.9670	**1.9654**
11	37.2230	46.4001	31.6987	21.9087	**0.9945**	2.0626	1.0189

Bold indicates the best values among all others in the same row (among all the methods)

Table 4 Absolute magnitude error over different frequency bands for 5th-order differentiator

Frequency range	Bartlett window	Hamming window	Minimax technique	Least-squares	L_1-method	PSO-L_1	BA-L_1
$[0, 0.2\pi]$	2.5069	2.0828	0.9966	0.3351	**0.0215**	0.2459	0.2012
$(0.2\pi, 0.4\pi]$	5.5755	3.2489	3.4999	0.8550	0.1728	0.1767	**0.1696**
$(0.4\pi, 0.6\pi]$	4.7006	1.2223	11.5684	1.7160	**0.2007**	0.2665	0.2757
$(0.6\pi, 0.8\pi]$	2.6962	3.5193	6.2456	2.7259	0.8100	**0.7351**	0.7462
$(0.8\pi, \pi]$	5.6070	2.0026	12.3805	**1.7941**	2.3098	1.8208	1.8447

Bold indicates the best values among all others in the same row (among all the methods)

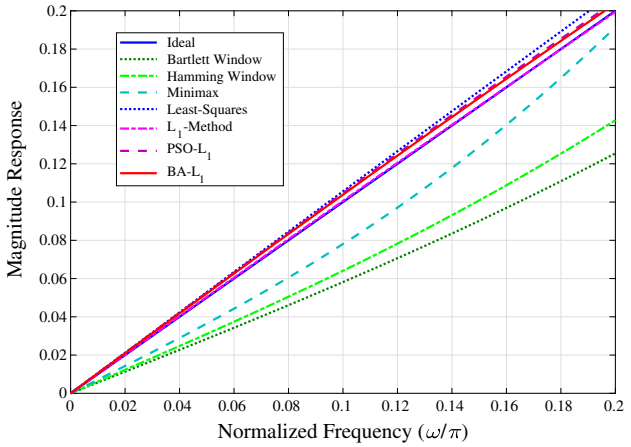

Fig. 4 Magnitude response of 5th-order FIR differentiator using different techniques for frequency range $[0, 0.2\pi]$

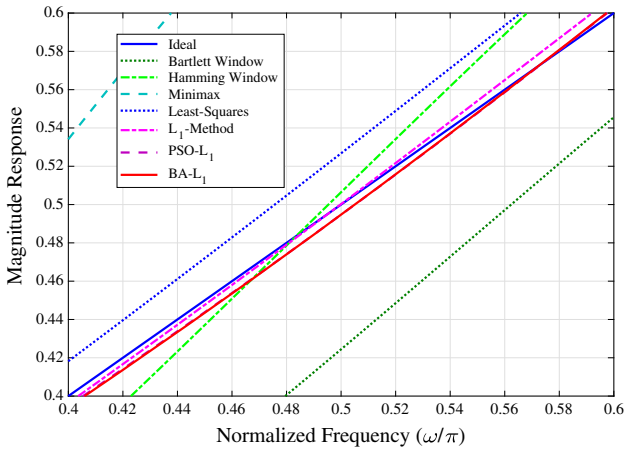

Fig. 5 Magnitude response of 5th-order FIR differentiator using different techniques for frequency range $[0.4\pi, 0.6\pi]$

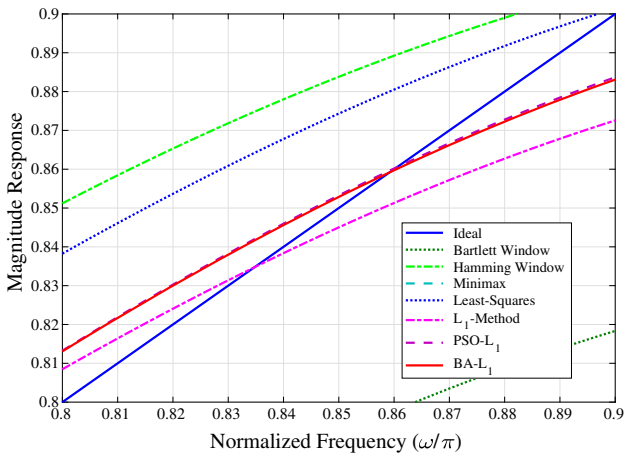

Fig. 6 Magnitude response of 5th-order FIR differentiator using different techniques for frequency range $[0.8\pi, 0.9\pi]$

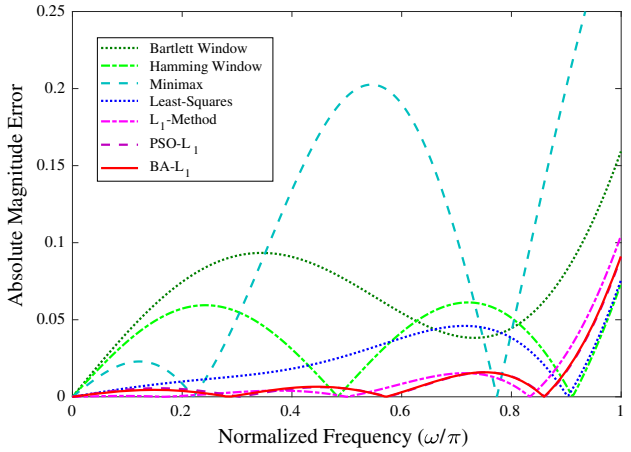

Fig. 7 Absolute magnitude error of 5th-order FIR differentiator using different techniques for complete digital frequency range

optimized (anti-symmetric filter coefficients, 3, 4 and 6, in this work). Specify the control parameters, A_i, r_i, $f_{\min}$, $f_{\max}$ and search space (upper and lower bound of filter coefficients).

Step 2: Initial Generation Generate initial bat population specifying their positions $x_i, i = 1, 2, \ldots, n$ and velocities v_i. Compute the fitness function, $F(x_i)$ to evaluate the effectiveness of every bat's position in search of the best solution.

Step 3: Movement After evaluating the fitness for every bat's position, the best location, known as the current global solution, x_j is selected. In the next iteration, update the new solutions, x_i^{l+1} and velocities, v_i^{l+1} using the following equations.

$$f_i = f_{\min} + (f_{\max} - f_{\min})\beta \tag{11}$$

$$v_i^{l+1} = v_i^l + (x_i^{l+1} - x_j)\, f_i \tag{12}$$

$$x_i^{l+1} = x_i^l + v_i^{l+1} \tag{13}$$

where β is a uniformly distributed random value in the range [0,1].

Step 4: Local Search If a random number $rand > r_i$, then select a solution among the best solutions. Else if $rand < r_i$, generate new solution for each bat using the random walk, given by

$$x_{\text{new}} = x_{\text{old}} + \epsilon A^l \tag{14}$$

where $\epsilon \in [-1, 1]$ and $A^l = \langle A_i^l \rangle$ is the average loudness for all the bats at the current iteration.

Step 5: Compare Compute fitness of the new solutions, $F(x_j)$. If $F(x_j) < F(x_i)$ and a random number $rand < A_i$, then retain the new solutions x_j as best solutions, otherwise goto step 3 until the maximum iterations are elapsed.

Table 5 Optimized coefficients of 7th-order FIR differentiator using different optimization techniques

Technique	$h(0) = -h(7)$	$h(1) = -h(6)$	$h(2) = -h(5)$	$h(3) = -h(4)$
Bartlett	0.00000000000001	0.02572332331877	0.08574441106258	− 0.38584984978161
Hamming	− 0.00514466466375	0.02279553116021	0.09638780923123	− 0.42965150895051
Minimax	0.05973220147459	− 0.06718840334105	− 0.01536497034256	0.42126651230326
Least-squares	0.00505881087707	− 0.00570234220811	− 0.02369872851383	0.42294670179145
L_1-method	− 0.00334537185986	0.02165812882307	− 0.10711915964935	1.23615231648740
PSO-L_1	− 0.00488445398081	0.01346792491689	− 0.04275095077928	0.40292314166423
BA-L_1	0.00508268272986	− 0.01362753783752	0.04291029638458	− 0.40348372383283

Step 6: Update The loudness, A_i, and pulse rate, r_i, are updated according to the following equations.

$$A_i^{l+1} = \alpha A_i^l \tag{15}$$

$$r_i^{l+1} = r_i^0[1 - \mathrm{e}^{-\gamma l}] \tag{16}$$

where $\alpha = \gamma = 0.8$ for the problem under consideration. Approaching the prey, loudness of bat decreases, whereas the pulse rate increases.

Step 7: Solution Record the best solution if the maximum number of iteration is exercised. Otherwise, go to step 3. The best solution corresponds to the minimum fitness function which is used to design the digital FIR differentiator.

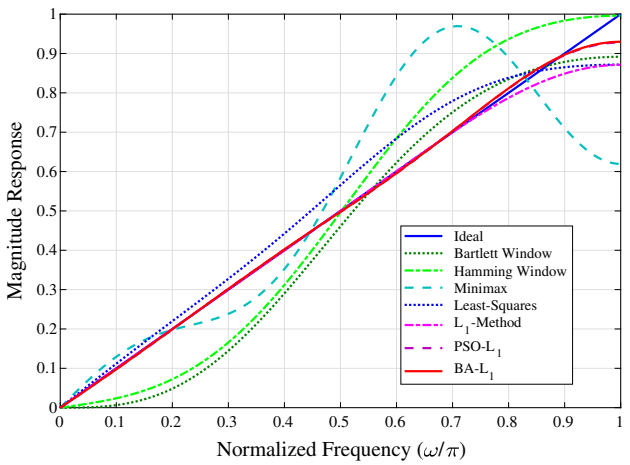

Fig. 8 Magnitude response of 7th-order FIR differentiator using different techniques over complete digital frequency range

4 Simulation and Analysis

This section presents simulation results and detailed analysis for the design of 5th-, 7th- and 11th-order FIR differentiator using the L_1-method, PSO-L_1 and BA-L_1. The simulation is performed on MATLAB using Intel Core i5, 2.53 GHZ, 4GB RAM PC. To affectively demonstrate the excellence of the proposed designs, comparative analysis is performed with the traditional window techniques, minimax method and the LS method. The digital differentiators are analyzed for different frequency bands in the complete frequency range. The values of controlling parameters of the L_1-algorithm, PSO-L_1 and BA-L_1 used for the design process are mentioned in Table 1.

4.1 Design Example 1: 5th-Order FIR Differentiator

In this example, we design a 5th-order FIR differentiator using the L_1-method, PSO-L_1 and BA-L_1. The optimized anti-symmetric filter coefficients obtained for the L_1-method, PSO-L_1, BA-L_1 along with the Bartlett and Hamming window technique, minimax method and LS design are given in Table 2. The magnitude response obtained using the window techniques, minimax, LS approach, the L_1-method, PSO-L_1 and BA-L_1 is shown in Fig. 3 for the complete frequency range. The observations for all the design algorithms on the measures of the absolute magnitude error

Table 6 Absolute magnitude error over different frequency bands for 7th-order differentiator

Frequency range	Bartlett window	Hamming window	Minimax technique	Least-squares	L_1-method	PSO-L_1	BA-L_1
$[0, 0.2\pi]$	5.4492	4.4837	1.1660	0.6907	**0.0014**	0.1100	0.1088
$(0.2\pi, 0.4\pi]$	9.2703	7.8976	3.0718	1.8096	**0.0063**	0.0986	0.1169
$(0.4\pi, 0.6\pi]$	2.8800	2.8336	6.3680	4.0823	**0.0242**	0.1692	0.1570
$(0.6\pi, 0.8\pi]$	2.7305	8.1168	14.6804	4.5994	**0.1874**	0.3102	0.3280
$(0.8\pi, \pi]$	2.5049	4.8768	12.0068	3.1504	3.6750	1.2789	**1.2547**

Bold indicates the best values among all others in the same row (among all the methods)

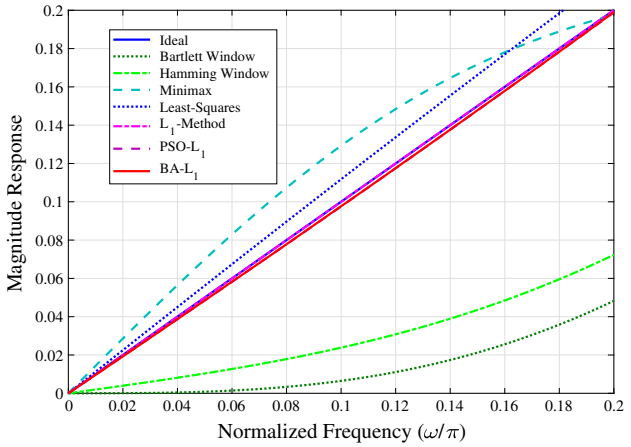

Fig. 9 Magnitude response of 7th-order FIR differentiator using different techniques for frequency range $[0, 0.2\pi]$

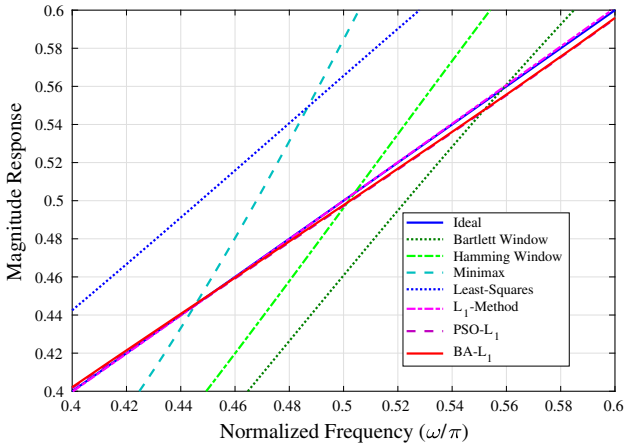

Fig. 10 Magnitude response of 7th-order FIR differentiator using different techniques for frequency range $[0.4\pi, 0.6\pi]$

for the frequency range $[0, \pi]$ are shown in Table 3. The absolute magnitude errors observed are 3.2373, 3.2451 and 3.5148 for the BA-L_1, PSO-L_1 and the L_1-method-based differentiator design, respectively. The performance of the algorithms is in the following order.

$$\text{BA} - L_1 > \text{PSO} - L_1 > L_1 - \text{method} > \text{LS} > \text{Hamming} > \text{Bartlett} > \text{Minimax}$$

In Table 4, detailed analysis on the basis of absolute magnitude error computed in different frequency bands is performed. For the frequency range $[0, 0.2\pi]$, performance of the L_1-method is best; for $\omega \in (0.2\pi, 0.4\pi]$, BA-$L_1$ yields least magnitude error; for $\omega \in (0.4\pi, 0.6\pi]$, the L_1-method performs better; for $\omega \in (0.6\pi, 0.8\pi]$, magnitude error for PSO-L_1 is minimum; and for $\omega \in (0.8\pi, \pi]$, the LS method gives comparable results to the proposed designs. The magnitude response for the 5th-order differentiator for the lower frequencies, mid-frequencies and higher frequencies is plotted in Figs. 4, 5 and 6, respectively. Furthermore, the absolute magnitude error for all the techniques with respect to the digital frequency is shown in Fig. 7. The observations made from tables and figures, and it can be inferred that the BA-L_1-based differentiator outperforms all other designs.

4.2 Design Example 2: 7th-Order FIR Differentiator

In the current example, the design of 7th-order FIR differentiator using the L_1-method, PSO-L_1 and BA-L_1 is demonstrated. Table 5 provides the optimized FIR filter coefficients incurred for the L_1-method, PSO-L_1, BA-L_1 and the Bartlett, Hamming window technique, minimax and LS designs. The comparison of magnitude response for the complete frequency range using all above mentioned approaches is presented in Fig. 8. It is observed from Table 3 that the

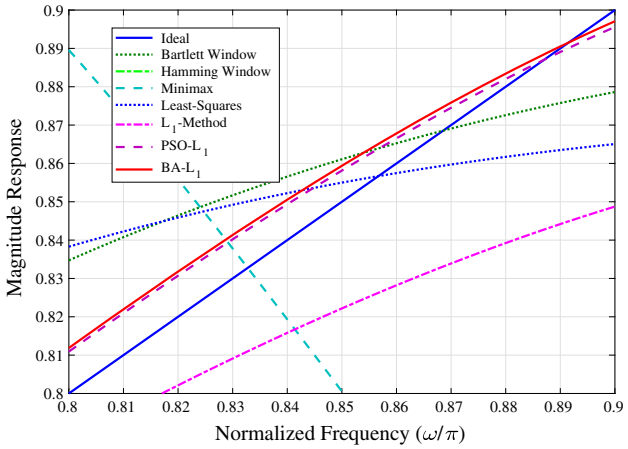

Fig. 11 Magnitude response of 7th-order FIR differentiator using different techniques for frequency range $[0.8\pi, 0.9\pi]$

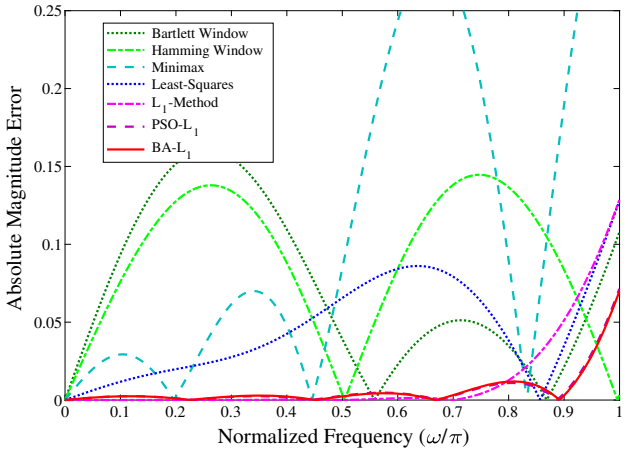

Fig. 12 Absolute magnitude error of 7th-order FIR differentiator using different techniques for complete digital frequency range

Table 7 Optimized coefficients of 11th-order FIR differentiator using different optimization techniques

Technique	$h(0) = -h(11)$ $h(3) = -h(8)$	$h(1) = -h(10)$ $h(4) = -h(7)$	$h(2) = -h(9)$ $h(5) = -h(6)$
Bartlett	0.00000000000001	− 0.00909410420360	− 0.02338483938070
Window	0.04910816269947	0.10912925044328	− 0.40923468916232
Hamming	0.00327387711329	− 0.00765385764298	− 0.02243775352578
Window	0.05451098603520	0.12622974006205	− 0.44177025622056
Minimax	0.05314225018098	− 0.06272950517185	0.01171440548398
	0.00277829612732	− 0.03188163305477	0.37375415617876
Least-squares	0.01078373236839	− 0.02398825025747	0.02598513367092
	−0.02074782575731	− 0.00897801193082	0.40810178597543
L_1-method	− 0.00289713205513	0.00978148970242	− 0.02110102887026
	0.04670470611281	− 0.13763330449670	1.26958159142235
PSO-L_1	0.00115836341259	− 0.00481968626529	0.00755658595232
	− 0.01270317896699	0.04013579745765	− 0.40437613250491
BA-L_1	0.00237548670700	− 0.00421312496658	0.00786459110191
	− 0.01560690807491	0.04449608535985	− 0.40456842610170

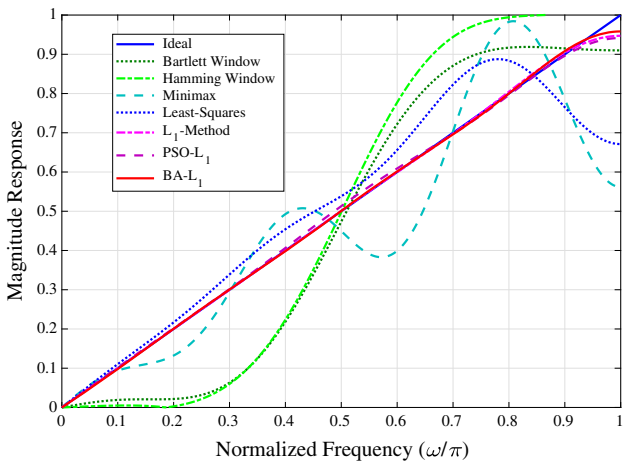

Fig. 13 Magnitude response of 11th-order FIR differentiator using different techniques over complete digital frequency range

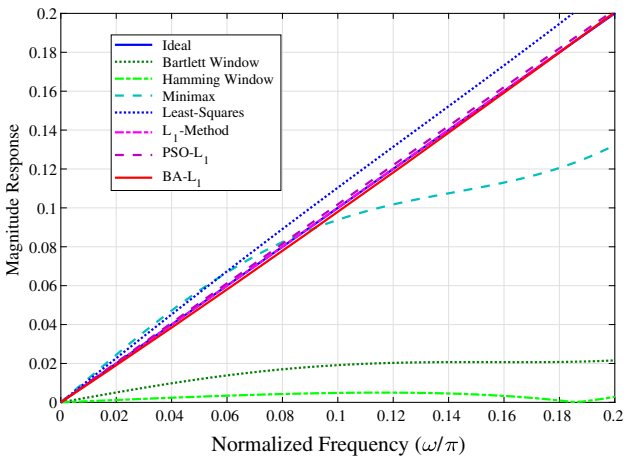

Fig. 14 Magnitude response of 11th-order FIR differentiator using different techniques for frequency range $[0, 0.2\pi]$

absolute magnitude error for the BA-L_1, PSO-L_1 and the L_1-method-based differentiator design is 1.9654, 1.9670 and 3.8943, respectively. The performance of the algorithms is in the following order.

$$\text{BA} - L_1 > \text{PSO} - L_1 > L_1 - \text{method} > \text{LS} > \text{Bartlett} > \text{Hamming} > \text{Minimax}$$

The absolute magnitude error is analyzed for different frequency bands and is presented in Table 6. In the frequency range $\omega \in [0, 0.2\pi]$, $(0.2\pi, 0.4\pi]$, $(0.4\pi, 0.6\pi]$ and $(0.6\pi, 0.8\pi]$, performance of the L_1-method is excellent and it yields the least magnitude error; and for $\omega \in (0.8\pi, \pi]$, the BA-L_1 design approach gives better results. The magnitude response for the 7th-order differentiator for the lower frequencies, mid-frequencies and higher frequencies is shown in Figs. 9, 10 and 11, respectively. Fig. 12 portrays the absolute magnitude error values for the complete frequency range. All the above observations conclude that the L_1-method-based differentiator design performs better among all other designs.

4.3 Design Example 3: 11th-Order FIR Differentiator

The design of 11th-order FIR differentiator using the L_1-method, PSO-L_1 and BA-L_1 is presented in this example. The anti-symmetric approximated filter coefficients are sequenced in Table 7. The magnitude response is plotted for the L_1-method, PSO-L_1, BA-L_1, LS approach, minimax, Bartlett, Hamming window technique in Fig. 13. The absolute magnitude error values given in Table 3 for the 11th-order differentiator is 1.0189, 2.0626 and 0.9945 for the BA-L_1,

Table 8 Absolute magnitude error over different frequency bands for 11th-order differentiator

Frequency range	Bartlett window	Hamming window	Minimax technique	Least-squares	L_1-method	PSO-L_1	BA-L_1
$[0, 0.2\pi]$	5.2284	6.0229	1.3444	0.5601	**0.0063**	0.0933	0.0801
$(0.2\pi, 0.4\pi]$	13.6896	13.9879	3.3605	2.3728	**0.0203**	0.1595	0.0652
$(0.4\pi, 0.6\pi]$	5.2491	5.9569	6.3077	2.7859	**0.0402**	0.7019	0.0969
$(0.6\pi, 0.8\pi]$	9.6551	14.1212	7.8577	6.5862	**0.1196**	0.2712	0.1752
$(0.8\pi, \pi]$	3.4009	6.3113	12.8284	9.5737	0.8081	0.8362	**0.6016**

Bold indicates the best values among all others in the same row (among all the methods)

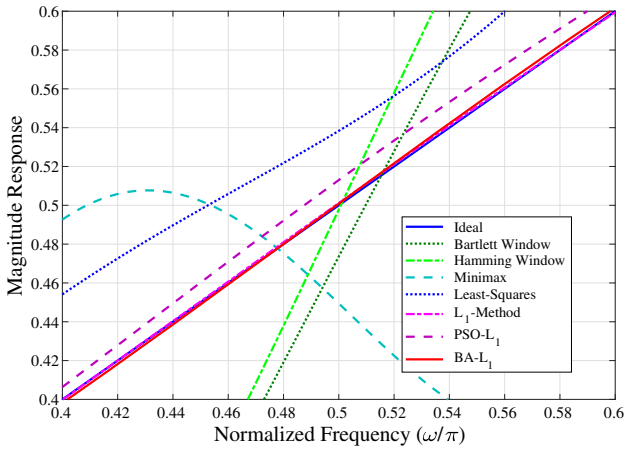

Fig. 15 Magnitude response of 11th-order FIR differentiator using different techniques for frequency range $[0.4\pi, 0.6\pi]$

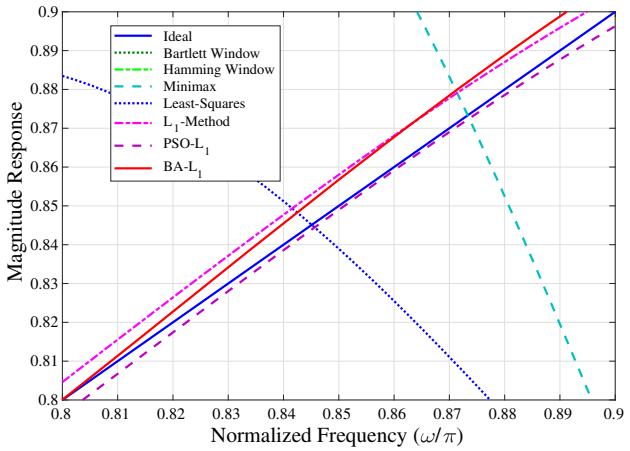

Fig. 16 Magnitude response of 11th-order FIR differentiator using different techniques for frequency range $[0.8\pi, 0.9\pi]$

PSO-L_1 and the L_1-method, respectively. The performance of the algorithms is in the following order.

$$L_1 - \text{method} > \text{BA} - L_1 > \text{PSO} - L_1 > \text{LS} > \text{Minimax} > \text{Bartlett} > \text{Hamming}$$

For the frequency range $\omega \in [0, 0.2\pi]$, $(0.2\pi, 0.4\pi]$, $(0.4\pi, 0.6\pi]$ and $(0.6\pi, 0.8\pi]$, the L_1-method outperforms all other design and with high accuracy yields the least magnitude error; for $\omega \in (0.8\pi, \pi]$, the BA-L_1 design method provides better results, as shown in Table 8. The magnitude response for the 11th-order differentiator for lower frequencies, mid-frequencies and higher frequencies is shown in Figs. 14, 15 and 16, respectively. In Fig. 17, the absolute magnitude error for the complete frequency range is depicted. From above results, it can be concluded that the absolute magnitude error is least for the L_1-method-based differentiator

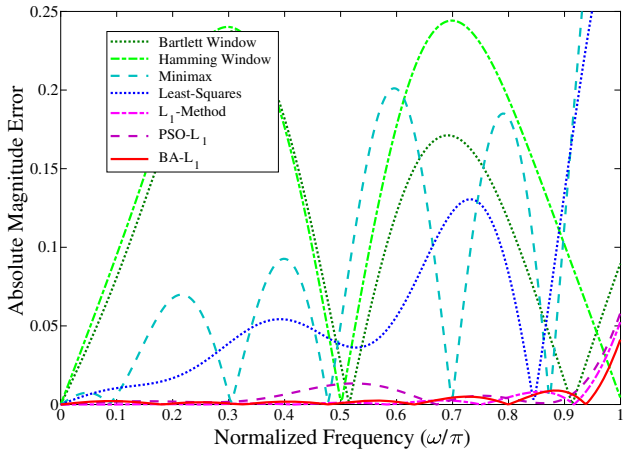

Fig. 17 Absolute magnitude error of 11th-order FIR differentiator using different techniques for complete digital frequency range

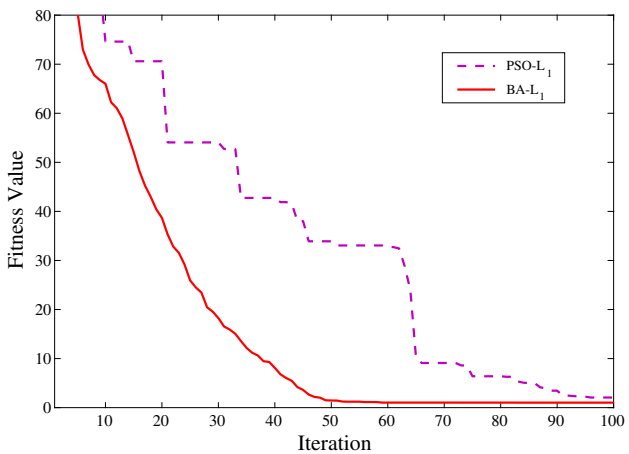

Fig. 18 Absolute magnitude error of 11th-order FIR differentiator using different techniques for complete digital frequency range

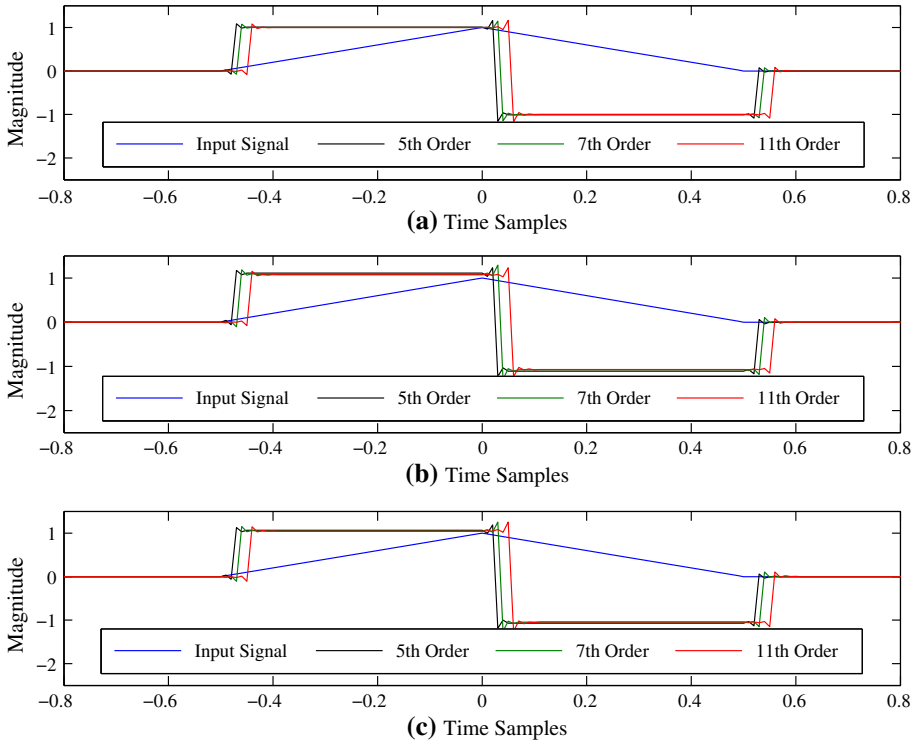

Fig. 19 Output response of the proposed differentiators using **a** the L_1-method, **b** PSO-L_1, **c** BA-L_1 for a triangular input pulse

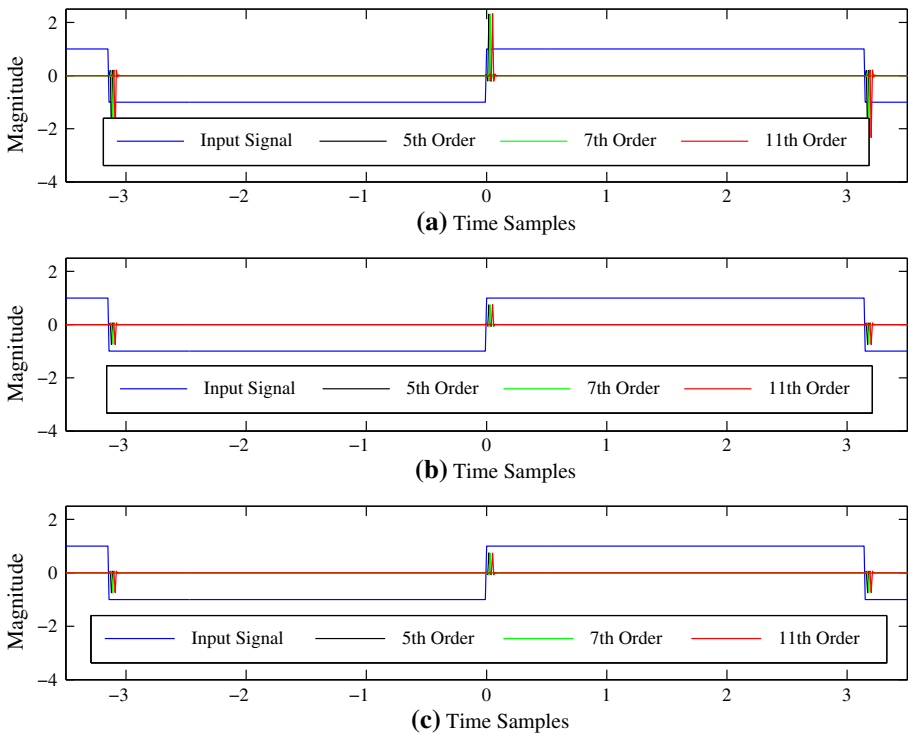

Fig. 20 Output response of the proposed differentiators using **a** the L_1-method, **b** PSO-L_1, **c** BA-L_1 for square input wave

design and the L_1-method outperforms other techniques at higher orders.

Fitness Profile The comparison of fitness curve for the optimization algorithms, PSO and BA is shown in Fig. 18. The bat algorithm converges to a lower value of magnitude error as compared to PSO. Moreover, the speed of convergence is observed to be faster for BA. This curve is plotted for the values obtained while simulating the 11th-order differentiator. Similar plots can be obtained for other designs.

Lastly, two digital input signals are considered to further verify the performance of the proposed differentiator designs and to prove them fit for real applications. Firstly, a triangular pulse of 1 s is provided as input wave; secondly, a square wave with 50% duty cycle is considered. Here, the input signals are filtered using the 5th-, 7th- and 11th-order differentiators designed using the L_1-method, PSO-L_1 and BA-L_1. Figure 19 depicts the output obtained with respect to the input triangular pulse when it is passed through the differentiators. The resulting square wave is featured with the group delay of 3, 4 and 6 samples with 5th-, 7th- and 11th-order differentiator, respectively. The differentiation of square wave, resulting into spikes at the pulse transition, is demonstrated in Fig. 20. Similar group delay is observed in the corresponding outputs. Hence, the feasibility of the proposed differentiator designs using the L_1-method, PSO-L_1 and BA-L_1 in real applications is confirmed.

5 Conclusion

The aim of this paper is to design a wideband digital FIR differentiator by utilizing the novel features of the L_1-method. A flat response is obtained over a wide frequency range for the design of 5th-, 7th- and 11th-order differentiator. The authors have made an attempt to further obtain optimized results by applying two swarm intelligence-based algorithms, PSO and BA. The results have been examined with the computation of relative magnitude error of the proposed designs with respect to the ideal response. To evaluate the efficient performance of the proposed method, detailed analysis has been carried out in different frequency bands. It can be concluded from these observation that the L_1-method, PSO-L_1 and BA-L_1 outperform other existing techniques considered for comparison window, minimax and LS method. Moreover, it is observed that the L_1-method is an improvement over all other designs for higher-order system. Finally, the proposed designs are tested on two input signals to verify the efficiency of response.

Here, the design of FIR differentiator with real coefficients is considered. However, complex coefficients value differentiator and Hilbert transformer can also be considered for further research.

References

1. Skolnik, M.I.: Introduction to Radar Systems. McGraw- Hill, New York (1980)
2. AL-Alaoui, M.A.: Novel FIR approximations of IIR differentiators with applications to image edge detection. In: Proceedings of the 18th IEEE International Conference on Electronics, Circuits and Systems (ICECS), 11–14 Dec 2011, Beirut, Lebanon (2011). https://doi.org/10.1109/ICECS.2011.6122335
3. Morgera, S.D.: Digital filtering and prediction for communications systems time synchronization. IEEE J. Ocean. Eng. **7**(3), 110–119 (1982)
4. Kumar, A.; Komaragiri, R.; Kumar, M.: From pacemaker to wearable: techniques for ECG detection systems. J. Med. Syst. **42**(2), 34 (2018)
5. Kumar, A.; Berwal, D.; Kumar, Y.: Design of High-performance ECG detector for implantable cardiac pacemaker systems using biorthogonal wavelet transform. Circuits Syst. Signal Process. (2018). https://doi.org/10.1007/s00034-018-0754-3
6. Laguna, P.; Thakor, N.V.; Caminal, P.; Jane, R.: Low-pass differentiator for biological signals with known spectra: application to ECG signal processing. IEEE Trans. Biomed. Eng. **37**(4), 420–425 (1990)
7. Kumar, M.; Rawat, T.K.: Fractional order digital differentiator design based on power function and least-squares. Int. J. Electron. **103**(10), 1639–1653 (2016)
8. Shaeen, K.; Elias, E.: Prototype filter design approaches for near perfect reconstruction cosine modulated filter banks—a review. J. Signal Process. Syst. **81**(2), 183–195 (2015)
9. Kumar, M.; Rawat, T.K.: Optimal fractional delay-IIR filter design using cuckoo search algorithm. ISA Trans. **59**, 39–54 (2015)
10. Kumar, M.; Rawat, T.K.: Optimal design of FIR fractional order differentiator using cuckoo search algorithm. Expert Syst. Appl. **42**, 3433–3449 (2015)
11. Al-Alaoui, M.A.: Novel digital integrator and differentiator. Electron. Lett. **29**(4), 376–378 (1993)
12. Bihan, J.L.: Novel class of digital integrators and differentiators. Electron. Lett. **29**(11), 971–973 (1993)
13. Al-Aloaui, M.A.: Novel IIR differentiator from the Simpson integration rule. IEEE Trans. Circuits Syst. I, Fundam. Theory Appl. **41**(2), 186–187 (1994)
14. Al-Aloaui, M.A.: Class of digital integrators and differentiators. IET Signal Process. **5**, 251–260 (2011)
15. Gupta, M.; Jain, M.; Kumar, B.: Recursive wideband digital integrator and differentiator. Int. J. Circuit Theory Appl. **39**, 775–782 (2011)
16. Papamarkos, N.; Chamzas, C.: A new approach for the design of digital integrators. IEEE Trans. Circuits Syst. I Fundam. Theory Appl. **43**(9), 785–791 (1996)
17. Ngo, N.Q.: A new approach for the design of wideband digital integrator and differentiator. IEEE Trans. Circuits Syst. II **53**(9), 936–940 (2006)
18. Karaboga, N.; Cetinkaya, B.: Design of digital FIR filters using differential evolution algorithm. Circuits Syst. Signal Process. **25**(5), 649–660 (2006)
19. Boudjelaba, K.; Ros, F.; Chikouche, D.: Potential of particle swarm optimization and genetic algorithms for FIR filter design. Circuits Syst. Signal Process. (2014). https://doi.org/10.1007/s00034-014-9800-y
20. Upadhyay, D.K.: Recursive wide band digital differentiators. IET Electron. Lett. **46**(25), 1661–1662 (2010)
21. Upadhyay, D.K.; Singh, R.K.: Recursive wide band digital differentiators and integrators. Electron. Lett. **47**(11), 647–648 (2011)
22. Jain, M.; Gupta, M.; Jain, N.: Linear phase second order recursive digital integrators and differentiators. Radio Eng. J. **21**(2), 712–717 (2012)
23. Gupta, M.; Relan, B.; Yadav, R.; Aggarwal, V.: Wideband digital integrators and differentiators designed using particle swarm optimization. IET Signal Process. **8**(6), 668–679 (2014)
24. Chang, W.D.; Chang, D.M.: Design of a higher-order digital differentiator using a particle swarm optimization approach. Mech. Syst. Signal Process. **22**(1), 233–247 (2008)
25. AL-Alaoui, M.A., Baydoun, M.: Novel wide band digital differentiators and integrators using different optimization techniques. In: Proceedings of the International Symposium on Signals, Cir-

cuits and Systems (ISSCS), 11–12 July 2013, Iasi, Romania (2013). https://doi.org/10.1109/ISSCS.2013.6651225
26. Rawat, T.K.: Digital Signal Processing, 1st edn. Oxford University Press, Oxford (2014)
27. Rice, J.R.: The Approximation of Functions, vol. I. Addison- Wesley, Boston (1964)
28. Bloomfield, P.: Least Absolute Deviations: Theory, Applications, and Algorithms. Birkhuser, Boston (1983)
29. Grossmann, L.D.; Eldar, Y.C.: An L_1-method for the design of linear-phase FIR digital filters. IEEE Trans. Signal Process. **55**(11), 5253–5266 (2007)
30. Aggarwal, A.; Rawat, T.K.; Kumar, M.; Upadhyay, D.K.: Optimal design of FIR high pass filter based on L_1 error approximation using real coded genetic algorithm. Eng. Sci. Technol. Int. J. **18**(4), 594–602 (2015)
31. Aggarwal, A.; Rawat, T.K.; Kumar, M.; Upadhyay, D.K.: Efficient design of digital FIR differentiator using L_1-method. RadioEngineering **25**(2), 86–92 (2016)
32. Aggarwal, A.; Kumar, M.; Rawat, T.K.: L_1 error criterion based optimal FIR filters. In: Annual IEEE India Conference (INDICON) (2014)
33. Aggarwal, A.; Rawat, T.K.; Kumar, M.; Upadhyay, D.K.: An L_1-method: application to digital symmetric type-II FIR filter design. In: Berretti, S., Thampi, S.M., Srivastava, P.R. (eds.) Intelligent Systems Technologies and Applications, pp. 335–343. Springer, Berlin (2016)
34. Aggarwal, A.; Kumar, M.; Rawat, T.K.; Upadhyay, D.K.: Design of optimal 2-D FIR differentiators with quadrantally symmetric properties using the L_1-method. In: International Conference on Signal Processing and Communication Systems, (ICSPCS'2016). (2016). https://doi.org/10.1109/ICSPCS.2016.7843369
35. Aggarwal, A.; Kumar, M.; Rawat, T.K.; Upadhyay, D.K.: Optimal design of 2-D FIR digital differentiator using L_1-norm based cuckoo-search algorithm. Multidimens. Syst. Signal Process. **28**(4), 1569–1587 (2017)
36. Yarlagadda, R.; Bednar, J.B.; Watt, T.L.: Fast algorithms for l_p deconvolution. IEEE Trans. Acoust. Speech Signal Process. **33**, 174–184 (1985)
37. Kennedy, J.; Eberhart, R.: Particle swarm optimization. Proc. IEEE Int. Conf. Neural Netw. **4**, 1942–1948 (1995)
38. Yang, X.S.: A New Metaheuristic Bat-Inspired Algorithm, Nature Inspired Cooperative Strategies for Optimization, vol. 284, pp. 65–74. Springer, Berlin (2010)
39. Zhang, J.W.; Wang, G.G.: Image matching using a bat algorithm with mutation. In: Du, Z.Y., Liu, B. (eds.) Applied Mechanics and Materials, vol. 203, no. 1, pp. 88–93. Trans Tech Publication, Switzerland (2012)
40. Kumar, M.; Aggarwal, A.; Rawat, T.K.: Bat algorithm: application to adaptive infinite impulse response system identification. Arab. J. Sci. Eng. **41**(9), 3587–3604 (2016)
41. Mishra, S.; Panda, M.: Bat algorithm for multilevel colour image segmentation using entropy-based thresholding. Arab. J. Sci. Eng. (2018). https://doi.org/10.1007/s13369-017-3017-x
42. Nakamura, R.Y.M.; Pereira, L.A.M.; Costa, K.A.; Rodrigues, D.; Papa, J.P.; Yang, X.S.: BBA: A binary bat algorithm for feature selection. In: Proceedings of the 25th SIBGRAPI Conference on Graphics, Patterns and Images, pp. 291–297. IEEE (2012). https://doi.org/10.1109/SIBGRAPI.2012.47
43. Mishra, S.; Shaw, K.; Mishra, D.: A new meta-heuristic bat inspired classification approach for microarray data. Procedia Technol. **4**, 802–806 (2012)
44. Yang, X.S.; He, X.: Bat algorithm: literature review and applications. Int. J. Bio Inspired Comput. **5**(3), 141–149 (2013)
45. Yang, X.S.; Gandomi, A.H.: Bat algorithm: a novel approach for global engineering optimization. Eng. Comput. **29**(5), 464–483 (2012)
46. Aggarwal, A.; Rawat, T.K.; Upadhyay, D.K.: Optimal design of L 1-norm based IIR digital differentiators and integrators using the bat algorithm. IET Signal Process. **11**(1), 26–35 (2017)
47. Gandomi, A.H.; Yang, X.S.; Alavi, A.H.; Talatahari, S.: Bat algorithm for constrained optimization tasks. Neural Comput. Appl. **22**(6), 1239–1255 (2013)